Available online at www.sciencedirect.com
SCIENCE DIRECT®
ELSEVIER
European Journal of Mechanics A/Solids 22 (2003) 801–814
EUROPEAN JOURNAL OF MECHANICS A/SOLIDS

Finite element analysis of the dynamic response of clamped sandwich beams subject to shock loading

X. Qiu, V.S. Deshpande, N.A. Fleck *

Cambridge University Engineering Department, Trumpington Street, Cambridge, CB2 1PZ, UK

Received 23 June 2003; accepted 1 September 2003

Abstract

The finite element (FE) method is employed to analyse the response of clamped sandwich beams subject to shock loadings. Pressure versus time histories representative of shock loadings are applied uniformly to the outer face of the sandwich beam; an impulse applied uniformly to the outer face of the sandwich beam is shown to model adequately shock loadings. Material elasticity and strain hardening representative of structural steels have only a minor effect upon the beam response. Further, the magnitude of the compressive strength of the core has only a limited influence upon the dynamic response of the sandwich beam for the representative range of core strengths considered. The FE results for the deflections and structural response time agree well with the rigid ideally-plastic analytical predictions of Fleck and Deshpande (J. Appl. Mech. (2003), in press).

Keywords: Sandwich beams; Dynamic plasticity; FE simulations

1. Introduction

Sandwich beams comprising stiff and strong face sheets and a low density core are commonly used in lightweight structures as they provide superior quasi-static bending strength to monolithic beams. The resistance of sandwich beams to dynamic loads remains to be fully investigated in order to quantify the advantages of sandwich construction over monolithic designs for application in shock resistant structures.

The response of the monolithic beams to shock type dynamic loadings has been investigated extensively over the past fifty years or so. Early work (at the time of World War II) included the full scale testing of monolithic plates and beams for a limited range of geometries and materials and the development of simple analytical models such as the 1D fluid–structure interaction model of Taylor (1941). Post World War II, a number of researchers have developed analytical models for the response of beams and plates subject to shock loadings using rigid plastic theory. In particular, Wang and Hopkins (1954) and Symmonds (1954) analysed the response of clamped axisymmetric plates and beams, respectively subject to impulsive loads. Both these studies were restricted to linear bending kinematics with in-plane stretching neglected. Jones (1971) extended the analysis of Symmonds (1954) by giving an approximate solution for the response of clamped beams under finite deflections. Readers are referred to Jones (1989) for an extensive review of the literature.

Recently, Xue and Hutchinson (2003) have carried out a 3D finite element (FE) investigation of the shock resistance of clamped sandwich beams with square honeycomb, corrugated and pyramidal cores. In these FE calculations, Xue and Hutchinson (2003) modelled the core topologies explicitly but ignored the fluid–structure interaction; a prescribed impulse was applied uniformly to the outer face of the sandwich beam. In a parallel study, Fleck and Deshpande (2003) proposed an analytical model for the response of sandwich beams subject to shock loadings including the effects of fluid–structure

* Corresponding author.
E-mail address: naf1@eng.cam.ac.uk (N.A. Fleck).

0997-7538/$ – see front matter
doi:10.1016/j.euromechsol.2003.09.002

interaction. They modelled the core as a smeared-out compressible solid which deforms at a constant plateau stress followed by lock-up at a densification strain. The analytical procedure demonstrated that sandwich beams offer superior resistance to shock loadings compared to monolithic beams of the same mass, especially for underwater shocks.

The main aim of the current study is to conduct FE calculations to explore the regime of validity of the approximate analytical model of Fleck and Deshpande (2003). First, the analysis of Fleck and Deshpande (2003) is summarised and the explicit finite element scheme briefly described. Second, we demonstrate via selected FE calculations that most shock loadings of sandwich beams may be approximated as impulsive loadings. Third, the accuracy of the ideally-plastic analytic model is evaluated for impulsive loading. The sensitivity of the FE predictions to material elasticity, strain hardening of the face sheet material and core strength is investigated in detail.

2. Review of an analytical model for the shock resistance of sandwich beams

Fleck and Deshpande (2003) developed an analytical model for the response of clamped sandwich beams subject to air and underwater shock loading. In this study we assess the accuracy of the analytical model with the effects of fluid–structure interaction neglected. In the limit of no fluid structure interaction, the analytical model assumes that the entire shock impulse I is transferred uniformly to the outer face of the sandwich beam and to the full section of the monolithic beam.

Clamped sandwich beams of span $2L$ are considered, with identical face sheets of thickness h and core thickness c, as shown in Fig. 1. The face sheets are assumed to be made from a rigid ideally-plastic material of yield strength σ_{fY}, density ρ_f and tensile failure strain ε_f. The core of density ρ_c is modelled as a compressive isotropic material with equal longitudinal and normal strengths σ_c: in uniaxial compression the core is assumed to deform at a constant stress σ_c with no lateral expansion up to a densification strain ε_D; beyond densification no further deformation is assumed to occur. Fleck and Deshpande (2003) split the response of the sandwich beam into three stages:

(i) Stage I – fluid–structure interaction phase, neglected here and considered no further;
(ii) Stage II – core compression phase;
(iii) Stage III – beam bending and stretching phase.

Stage II – core compression phase. The impulse I per unit area imparts a velocity $v_o = I/(\rho_f h)$ to the outer face. The outer face compresses the core, and the core compressive strength σ_c, decelerates the outer face and simultaneously accelerates the inner face. The final common velocity of the faces and the core is dictated by momentum conservation and the ratio ψ of the energy lost U_{lost} in this phase to the initial kinetic energy $I^2/(2\rho_f h)$ of the outer face is given by

$$\psi = \frac{1+\hat{\rho}}{2+\hat{\rho}}, \tag{1}$$

where $\hat{\rho} = \rho_c c/(\rho_f h)$ is the ratio of the mass of the core to the mass of one face sheet. This energy lost is dissipated by plastic dissipation in compressing the core and thus the core compression strain ε_c in this stage is given by

$$\varepsilon_c = \frac{\bar{I}^2}{2\bar{\sigma}\bar{c}^2\bar{h}}\frac{\bar{h}+\bar{\rho}}{2\bar{h}+\bar{\rho}}, \tag{2}$$

where $\bar{h} \equiv h/c$, $\bar{c} \equiv c/L$, $\bar{\rho} \equiv \rho_c/\rho_f$, $\bar{I} \equiv I/(L\sqrt{\sigma_{fY}\rho_f})$ and $\bar{\sigma} \equiv \sigma_c/\sigma_{fY}$. However, if U_{lost} is too high such that ε_c as given by (2) exceeds the densification strain ε_D, then ε_c is set to the value ε_D and the analytical analysis does not account for the

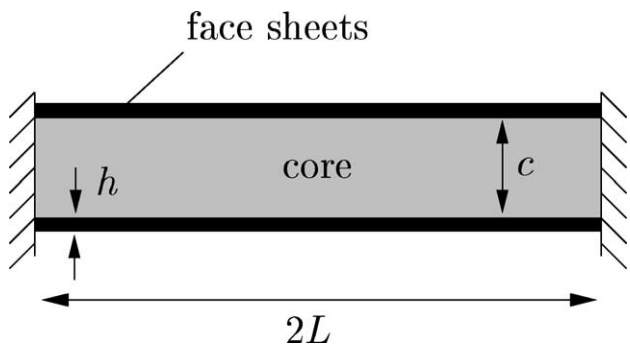

Fig. 1. Geometry of the sandwich beam.

additional dissipation mechanisms required to conserve energy. After the core has compressed to the strain ε_c, the core height is reduced to $(1-\varepsilon_c)c$. An approximate estimate of the time T_c of this phase (calculated by neglecting the mass of the core) is given by

$$\overline{T}_c \equiv \frac{T_c}{L\sqrt{\rho_f/\sigma_{fY}}} = \begin{cases} \dfrac{\bar{I}}{2\bar{\sigma}}, & \text{if } \bar{I}^2 < 4\bar{\sigma}\bar{c}^2\bar{h}\varepsilon_D \\ \dfrac{\bar{I}}{2\bar{\sigma}}\left[1-\sqrt{1-\dfrac{4\bar{\sigma}\bar{c}^2\bar{h}\varepsilon_D}{\bar{I}^2}}\right], & \text{otherwise.} \end{cases} \tag{3}$$

Typically, the core compression time T_c is small compared to the structural response time, and thus the transverse deflection of the inner face of the sandwich beam in this stage can be neglected.

Stage III – beam bending and stretching phase. At the end of Stage II, the sandwich beam has a uniform velocity except for a boundary layer near the supports. The beam is brought to rest by plastic bending and stretching. This problem has been investigated by a number of researchers as mentioned in Section 1. Fleck and Deshpande (2003) extended these analyses and presented a solution that is valid in both the small and large deflection regimes. They approximated the yield surface of the sandwich beam under bending moment M and axial load N to be either inscribing or circumscribing squares to the actual yield locus as sketched in Fig. 2(a). Employing the circumscribing yield locus, the maximum transverse deflection of inner face of the sandwich beam at its mid-span and the time T required to achieve this deflection are given by

$$\overline{w} \equiv \frac{w}{L} = \frac{\alpha_2}{2}\left[\sqrt{1+\frac{8\bar{I}^2\alpha_3}{3\alpha_1\alpha_2}}-1\right], \tag{4a}$$

and

$$\overline{T} \equiv \frac{T}{L\sqrt{\rho_f/\sigma_{fY}}} = \frac{\alpha_2}{2}\frac{\bar{c}(2\bar{h}+\bar{\rho})}{\bar{I}}\left[\sqrt{1+\frac{4\bar{I}^2\alpha_3}{3\alpha_1\alpha_2}}-1\right]+\sqrt{\frac{\bar{c}(2\bar{h}+\bar{\rho})}{3\hat{c}(2\hat{h}+\bar{\sigma}\bar{c}/\hat{c})}}\tan^{-1}\left[4\bar{I}\sqrt{\frac{\alpha_3}{3\alpha_1\alpha_2+4\bar{I}^2\alpha_3}}\right], \tag{4b}$$

respectively, where

$$\alpha_1 = \hat{c}^3\left[(1+2\hat{h})^2-1+\bar{\sigma}\bar{c}/\hat{c}\right](1+2\hat{h})\bar{c}(\bar{\rho}+2\bar{h}), \tag{5a}$$

$$\alpha_2 = \frac{\hat{c}[(1+2\hat{h})^2-1+\bar{\sigma}\bar{c}/\hat{c}]}{2\hat{h}+\bar{\sigma}\bar{c}/\hat{c}}, \quad \text{and} \tag{5b}$$

$$\alpha_3 = \hat{c}(1+2\hat{h}). \tag{5c}$$

The above equations are in terms of the non-dimensional geometric variables of the sandwich beam

$$\bar{c} \equiv \frac{c}{L}, \quad \bar{h} \equiv \frac{h}{c}, \quad \hat{c} \equiv \bar{c}(1-\varepsilon_c), \quad \text{and} \quad \hat{h} \equiv \frac{\bar{h}}{1-\varepsilon_c}. \tag{6}$$

Alternatively, for the choice of the inscribing yield locus the corresponding relations for the deflection and structural response time are

$$\overline{w} \equiv \frac{w}{L} = \frac{\alpha_2}{2}\left[\sqrt{1+\frac{16\bar{I}^2\alpha_3}{3\alpha_1\alpha_2}}-1\right], \tag{7a}$$

and

$$\overline{T} \equiv \frac{T}{L\sqrt{\rho_f/\sigma_{fY}}} = \frac{\alpha_2}{2}\frac{\bar{c}(2\bar{h}+\bar{\rho})}{\bar{I}}\left[\sqrt{1+\frac{8\bar{I}^2\alpha_3}{3\alpha_1\alpha_2}}-1\right]+\sqrt{\frac{2\bar{c}(2\bar{h}+\bar{\rho})}{3\hat{c}(2\hat{h}+\bar{\sigma}\bar{c}/\hat{c})}}\tan^{-1}\left[4\bar{I}\sqrt{\frac{\alpha_3}{3\alpha_1\alpha_2/2+4\bar{I}^2\alpha_3}}\right], \tag{7b}$$

respectively. Fleck and Deshpande (2003) state a failure criterion for the sandwich beam based on an estimate of the tensile strain in the face sheets of the sandwich beam, assuming uniform stretching of the entire face sheet. The tensile strain ε in the face sheets is approximately $\frac{1}{2}\overline{w}^2$; setting this strain equal to the tensile ductility ε_f of the face sheet material, the maximum impulse $\bar{I}_c$ sustained by the sandwich beams is given by

$$\bar{I}_c = \sqrt{\frac{3\alpha_1\alpha_2}{8\alpha_3}\left[\left(\frac{2\sqrt{2\varepsilon_f}}{\alpha_2}+1\right)^2-1\right]}, \tag{8a}$$

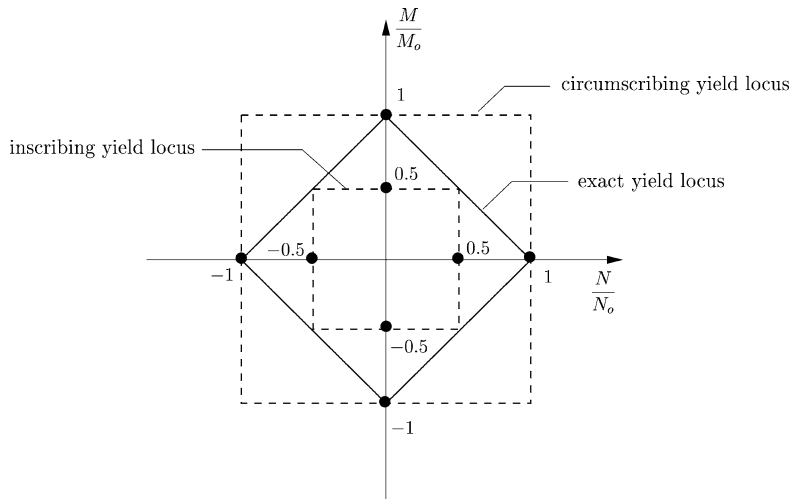

(a)

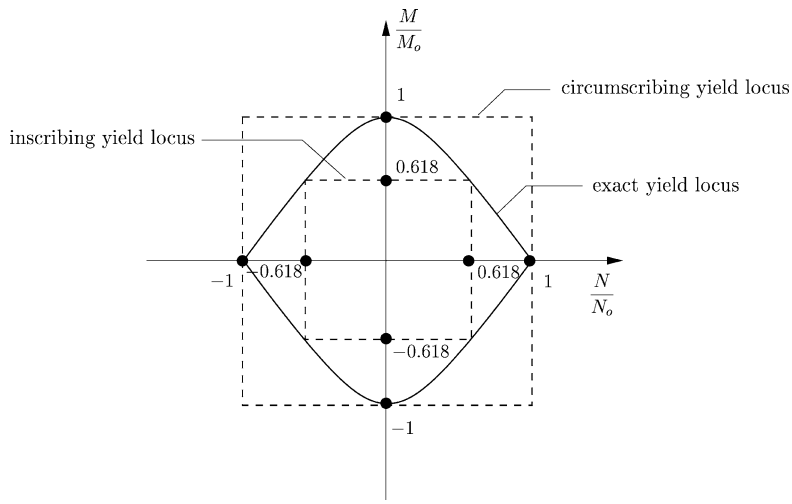

(b)

Fig. 2. Sketches of the exact, inscribing and circumscribing yield loci of (a) the sandwich beam and (b) the monolithic beam. Here M_o and N_o are the fully plastic bending moments and axial loads, respectively of the beams.

if the circumscribing yield locus is employed and

$$\bar{I}_c = \sqrt{\frac{3\alpha_1\alpha_2}{16\alpha_3}\left[\left(\frac{2\sqrt{2\varepsilon_f}}{\alpha_2}+1\right)^2-1\right]}, \tag{8b}$$

for the inscribing yield locus.

Similar expressions exist for the deflection and structural response time, see Fleck and Deshpande (2003). For monolithic beams, there is no core compression and the analysis reduces only to that of Stage III of the deformation history described above. The maximum deflection w of the mid-span of a monolithic beam of thickness h and span $2L$, and the time T to attain this deflection are given by

$$\overline{w} = \frac{h}{2L}\left[\sqrt{1+\frac{8\bar{I}^2}{3}\left(\frac{L}{h}\right)^4}-1\right] \quad \text{and} \tag{9a}$$

$$\overline{T} = \frac{1}{2\bar{I}}\left(\frac{h}{L}\right)^2\left[\sqrt{1+\frac{4}{3}\bar{I}^2\left(\frac{L}{h}\right)^4}-1\right]+\frac{1}{\sqrt{3}}\tan^{-1}\left[\frac{2\bar{I}(L/h)^2}{\sqrt{3+4\bar{I}^2(L/h)^4}}\right], \tag{9b}$$

respectively, if a circumscribing yield locus as sketched in Fig. 2(b) is employed and by

$$\overline{w} = \frac{h}{2L}\left[\sqrt{1 + \frac{8\bar{I}^2}{3 \times 0.618}\left(\frac{L}{h}\right)^4} - 1\right] \quad \text{and} \tag{10a}$$

$$\overline{T} = \frac{1}{2\bar{I}}\left(\frac{h}{L}\right)^2\left[\sqrt{1 + \frac{4}{3 \times 0.618}\bar{I}^2\left(\frac{L}{h}\right)^4} - 1\right] + \frac{1}{\sqrt{3 \times 0.618}}\tan^{-1}\left[\frac{2\bar{I}(L/h)^2}{\sqrt{3 \times 0.618 + 4\bar{I}^2(L/h)^4}}\right], \tag{10b}$$

if the inscribing yield locus (Fig. 2(b)) is used instead.

3. Numerical results

Comparisons of the finite element (FE) and analytical predictions of the response of the monolithic and sandwich beams are discussed in this section. Unless otherwise specified, the face sheets of the sandwich beam are assumed to be made from an elastic ideally plastic solid with a yield strength σ_{fY}, a yield strain ε_{fY}, and density ρ_f. The Young's modulus is specified by $E_f \equiv \sigma_{fY}/\varepsilon_{fY}$. This solid is modelled as J2 flow theory solid. No attempt is made to model the micro-structure of the sandwich core explicitly as has been done in Xue and Hutchinson (2003). Instead, in line with the analysis of Fleck and Deshpande (2003), the core is modelled as a compressible continuum using the foam constitutive model developed by Deshpande and Fleck (2000). This constitutive law employs an isotropic yield surface specified by

$$\hat{\sigma} - \sigma_c = 0, \tag{11a}$$

where the equivalent stress is defined by

$$\hat{\sigma}^2 \equiv \frac{1}{1 + (\alpha/3)^2}\left[\sigma_e^2 + \alpha^2\sigma_m^2\right]. \tag{11b}$$

Here, $\sigma_e \equiv \sqrt{3 s_{ij} s_{ij}/2}$ is the von-Mises effective stress with s_{ij} the deviatoric stress tensor and $\sigma_m \equiv \sigma_{kk}/3$, the mean stress. The yield strength σ_c is specified as a function of the equivalent plastic strain using uniaxial compression stress versus strain data. Normality of plastic flow is assumed which implies that the plastic Poisson's ratio $\nu_p = -\dot{\varepsilon}^p_{22}/\dot{\varepsilon}^p_{11}$ corresponding to uniaxial compression in the 1-direction is given by

$$\nu_p = \frac{1/2 - (\alpha/3)^2}{1 + (\alpha/3)^2}. \tag{12}$$

The reference material properties for the sandwich beam were taken to be as follows. The face sheets were assumed to be made out of a stainless steel with a yield strength $\sigma_{fY} = 500$ MPa, yield strain $\varepsilon_{fY} = 0.2\%$, an elastic Poisson's ratio $\nu = 0.3$ and a material density $\rho_f = 8000$ kg·m^{-3}. The core properties are taken to be representative of a lattice material such as the pyramidal core (Deshpande and Fleck, 2001) made from the same solid material as the face sheets. Thus, the isotropic core yield strength is taken to be

$$\sigma_c = 0.5\bar{\rho}\sigma_{fY}, \tag{13}$$

where $\bar{\rho} \equiv \rho_c/\rho_f$ is the relative density of the core. As the reference case, we take $\bar{\rho} = 0.1$ (i.e. core density $\rho_c = 800$ kg·m^{-3}) with $\alpha = 3/\sqrt{2}$ giving a plastic Poisson's ration $\nu_p = 0$. The plastic crush strength σ_c of the foam core was taken to be independent of the effective plastic strain up to a densification strain $\varepsilon_D = 0.5$: beyond densification, a linear hardening behaviour with a very large tangent modulus $E_t \approx 0.2E_f$ was assumed. Further, the core was assumed to be elastically isotropic with a yield strain $\varepsilon_{cY} = 0.2\%$ and an elastic Poisson's ratio $\nu_c = 0$.

All computations were performed using the explicit time integration version of the commercially available finite element code ABAQUS version 6.2. Symmetry about the mid-span of the beam was assumed and the beam was modelled using four noded plane strain quadrilateral elements with reduced integration (element type *CPE4R* in the ABAQUS notation). Numerical damping associated with volumetric straining in ABAQUS explicit was switched off by setting the bulk viscosity associated with this damping to zero; using the default viscosity in ABAQUS results in substantial artificial viscous dissipation due to the large volumetric compression of the core. For a typical beam of geometry $\bar{c} = 0.03$ and $\bar{h} = 0.1$, there were 2 and 8 elements through the thickness of the face sheets and core, respectively, and 100 elements along half the beam length L. Mesh sensitivity studies revealed that further refinements did not improve the accuracy of the calculations appreciably.

3.1. Impulsive versus finite pressure loading

Consider a clamped sandwich beam of length $2L$ with identical face sheets of thickness h and a core of thickness c. The plastic bending moment M_p of this beam is given by

$$M_p = \frac{\sigma_{fY}(c+2h)^2}{4} - \frac{\sigma_{fY}c^2}{4} + \frac{\sigma_c c^2}{4}, \tag{14}$$

and thus the static collapse pressure p_c of this beam, subject to a uniformly distributed load, is

$$\frac{p_c}{\sigma_{fY}} = \bar{c}^2\big[(1+2\bar{h})^2 - 1 + \bar{\sigma}\big]. \tag{15}$$

For a representative sandwich beam with $\bar{c} = 0.03$, $\bar{h} = 0.1$ and $\bar{\sigma} = 0.05$ made from a steel with $\sigma_{fY} = 500$ MPa, the static collapse pressure is $p_c \approx 0.22$ MPa.

Now consider shock loading of this sandwich beam. The shock wave due to the detonation of a high explosive either in air or water results in an exponentially decaying pressure versus time history with a peak pressure p_o on the order of 100 MPa and a decay constant $\theta \approx 0.1$ ms; see Cole (1948) and Swisdak (1978) for summaries of the main phenomena associated with shock waves due to explosions. The peak pressure p_o due to shock loading is much greater than the static collapse pressure p_c of the clamped sandwich beam. Jones (1989) argued that for $\eta = p_o/p_c > 10$, dynamic loading with a pressure versus time history $p(t)$ can be treated as impulsive with an impulse I of magnitude

$$I = \int_0^\infty p(t)\,\mathrm{d}t, \tag{16}$$

without any substantial loss of accuracy for monolithic beams. Thus, shock loading of a monolithic beam is often assumed to be impulsive. We proceed to verify this assertion for sandwich beams.

Consider a representative sandwich beam with the reference material properties as specified above and geometry $\bar{c} = 0.03$ and $\bar{h} = 0.1$. We now consider the finite element predictions of the response of the beam subjected to a uniformly distributed pressure with a pressure versus time history

$$p = \begin{cases} p_o & \text{if } 0 \leqslant t \leqslant \tau, \\ 0 & \text{otherwise,} \end{cases} \tag{17}$$

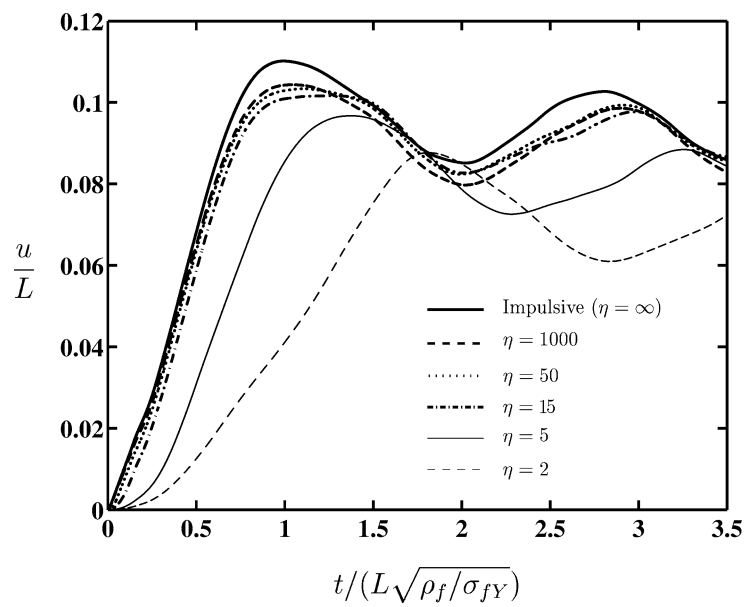

Fig. 3. Response of sandwich beams ($\bar{c} = 0.03$, $\bar{h} = 0.1$) with reference material properties, subject to a pressure versus time loadings corresponding to a normalised impulse $\bar{I} = 10^{-3}$.

such that the impulse $I = p_o\tau$. The sensitivity of the normalised transverse displacement u/L at the mid-span of the inner face sheet to the dynamic pressure ratio η is explored in Fig. 3, for a fixed impulse $\bar{I} \equiv I/(L\sqrt{\sigma_{fY}\rho_f}) = 10^{-3}$. Each curve gives u/L as a function of normalised time $t/(L\sqrt{\sigma_{fY}/\rho_f})$, at selected values of η. The limiting case of impulsive loading is included in Fig. 3: in the FE calculation the outer face sheet is given a uniform velocity v_o defined by

$$v_o = \frac{\bar{I}}{\bar{c}\bar{h}}\sqrt{\frac{\sigma_{fY}}{\rho_f}}. \tag{18}$$

For all practical purposes, $\eta \geqslant 15$ is equivalent to impulsive loading. Thus, as assumed from the outset in the Fleck and Deshpande (2003) analysis, typical air and water shock loadings can be approximated as impulsive loading of the sandwich beams. In the following, the finite element method is employed to investigate the response of monolithic and sandwich beams to impulsive loadings.

3.2. Comparison of finite element and analytical predictions

Comparisons of the FE results and analytical predictions of Fleck and Deshpande (2003) for the uniform impulsive loading of clamped monolithic and sandwich beams are presented in this section. In particular, comparisons are presented for:

(i) The maximum mid-span deflection w of the inner face of the sandwich beam. This is defined as the peak in the displacement versus time trace as shown in Fig. 3.
(ii) The structural response time T, defined as the time taken to reach this maximum deflection.
(iii) Core compression ε_c, defined as the maximum nominal strain in the core at mid-span of the beam.
(iv) Core compression time T_c, defined as the time taken to attain the core compression ε_c.

3.2.1. Impulsive loading of monolithic beams

The focus of the present study is the analysis of sandwich beams. However, for reference purposes we begin with a brief comparison of FE and analytical predictions for the response of monolithic beams. Here we focus on the response of slender beams where the bending deflections dominate; shear deflections become increasingly important for stubby beams and these cases are not analysed here; see Jones (1989) for a detailed discussion on the dynamic shearing of monolithic beams.

Consider a slender monolithic beam of thickness h and length $2L$ made from the same material as the face sheets of the sandwich beam; i.e., an elastic perfectly-plastic solid with a yield strength $\sigma_{fY} = 500$ MPa, yield strain $\varepsilon_{fY} = 0.2\%$, an elastic Poisson's ratio $\nu = 0.3$ and a material density $\rho_f = 8000$ kg·m^{-3}. The dependence of the normalised maximum deflection $\overline{w}$ of the mid-span of the beam upon the uniformly applied normalised impulse $\bar{I}$ is shown in Fig. 4(a), for a beam with aspect ratio $L/h = 50$. Analytical predictions of this maximum deflection employing the circumscribing and inscribing yield surfaces are included in Fig. 4(a): while the inscribing yield surface predictions are in good agreement with the FE results over the range of impulses investigated here, the circumscribing yield surface model underpredicts the deflections. The analytical and FE predictions of the normalised structural response time $\overline{T}$, as functions of the applied normalised impulse $\bar{I}$ are given in Fig. 4(b). For the range of impulses considered here the monolithic beam behaves like a stretched string and the structural response time is approximately independent of magnitude of the impulse. It is seen that the FE predictions of the structural response time T are in good agreement with the analytical model employing the circumscribing yield locus.

3.2.2. Impulsive loading of sandwich beams

Dynamic finite element simulations and analytical predictions have been performed on sandwich beams made from the reference materials specified above. The comparisons between the analytical and FE predictions are carried out in two stages. First, for a fixed impulse the response of the sandwich beams is investigated as function of the beam geometry and second, the response of a sandwich beam with a representative geometry is studied for varying levels of impulse.

For the purposes of selecting appropriate sandwich beam geometries for the FE calculations, we plot a design chart for sandwich beams subjected to a normalised impulse $\bar{I} = 10^{-3}$ and with an assumed face sheet material ductility $\varepsilon_f = 0.2$. The design chart shown in Fig. 5 has been constructed using the analytical model with the circumscribing yield locus. Contours of the maximum normalised deflection $\overline{w}$ of the mid-span of the inner face of the sandwich beams along with the regime of tensile failure of the face sheet are shown on the chart. Twelve beam geometries with $0.03 \leqslant \bar{h} \leqslant 0.3$ and $0.01 \leqslant \bar{c} \leqslant 0.06$ (as indicated in Fig. 5) are selected for the FE calculations. This range of beam geometries represents most practical beam geometries, and the analytic predictions for the mid-span displacements of the inner face of the sandwich beam are in the range $0.01 \leqslant \overline{w} \leqslant 0.2$.

Comparisons of the FE and analytical predictions (inscribing yield locus) for $\overline{w}$ and core compression ε_c as functions of $\bar{h}$ are shown in Figs. 6(a) and 6(b), respectively for $\bar{c} = 0.03$ and $\bar{c} = 0.04$, with $\bar{I} = 10^{-3}$. Similarly, Figs. 7(a) and 7(b) show comparisons of the analytical and FE predictions of $\overline{w}$ and ε_c versus $\bar{c}$ for beams with $\bar{h} = 0.06$ and 0.2. In all of the above

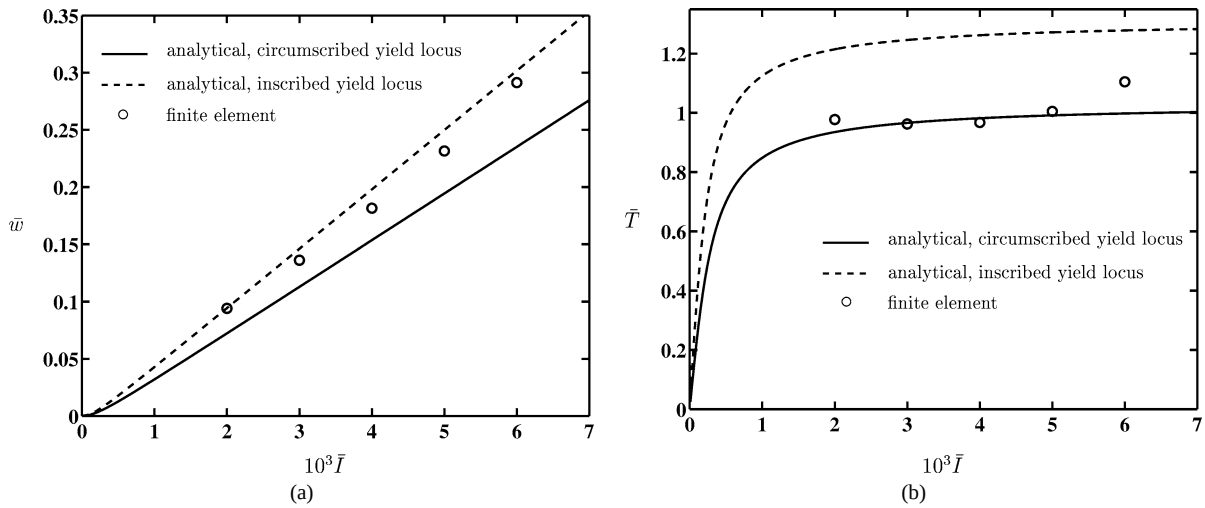

Fig. 4. A comparison of between analytical and FE predictions of the (a) maximum deflection at the mid-span and (b) structural response time, of a monolithic beam with aspect ratio $L/h = 50$ as a function of the applied impulse.

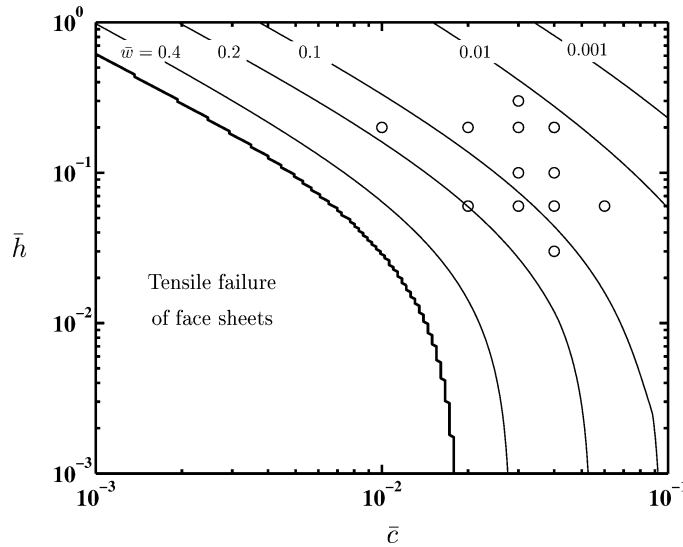

Fig. 5. Design chart for a clamped sandwich beam with a core of strength $\bar{\sigma} = 0.05$ and a densification strain $\varepsilon_D = 0.5$, and a face sheet material of ductility $\varepsilon_f = 0.2$ subject to a normalised impulse $\bar{I} = 10^{-3}$. Contours of the maximum normalised deflection $\overline{w}$ of the mid-span of the inner face sheet of the sandwich beam are included in the chart. The symbols denote the sandwich beam geometries selected for FE calculations.

cases good agreement is seen between the analytical and FE predictions, with the discrepancy between the analytical and FE predictions not exceeding 5%. As in the monolithic beam case, the analytical model employing the circumscribing yield locus underpredicts the deflections.

Next consider a representative sandwich beam of geometry, $\bar{c} = 0.03$ and $\bar{h} = 0.1$, subject to impulses in the range $7.5 \times 10^{-4} \leqslant \bar{I} \leqslant 3.2 \times 10^{-3}$. A comparison of the FE and analytical predictions of the maximum deflection $\overline{w}$ of the inner face sheet versus $\bar{I}$ and core compression ε_c versus $\bar{I}$ are shown in Figs. 8(a) and 8(b), respectively. While the analytical predictions employing the inscribing yield surface capture the beam deflections reasonably accurately at low impulses, at higher impulses the analytical model overpredicts the deflections. Similarly, Fig. 8(b) shows that the analytical calculation also substantially overpredicts the core compression in the high impulse domain. These discrepancies can be rationalised by recalling that the analytical model neglects the reduction in momentum due to an impulse provided by the supports in the core compression phase. With increasing impulse this assumption is no longer valid as the higher core compression gives rise to significant stretching of

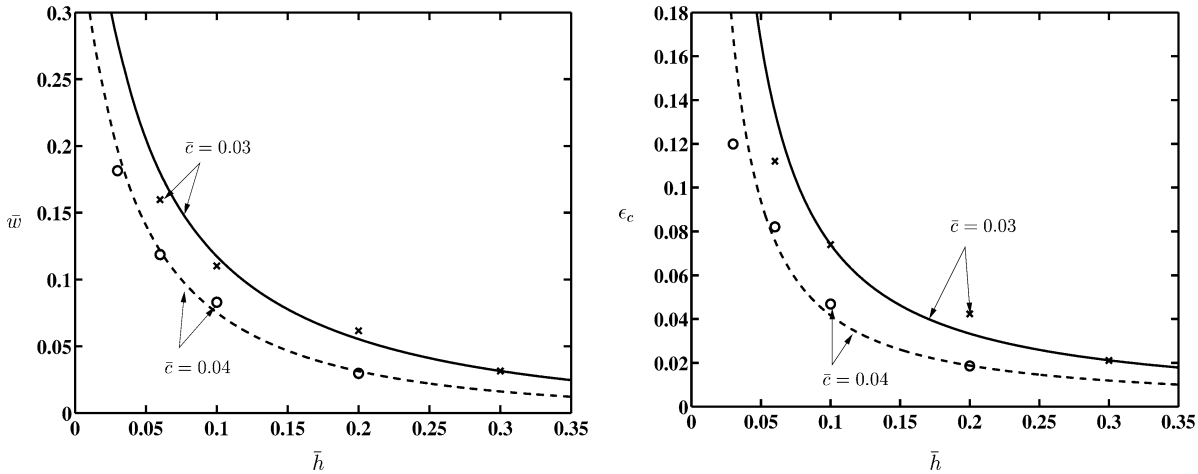

Fig. 6. A comparison between analytical and FE predictions of the (a) maximum deflection $\overline{w}$ at the mid-span of the inner face sheet and (b) core compression ε_c of sandwich beams with reference material properties subject to a normalised impulse $\bar{I} = 10^{-3}$. Analytical predictions employing the inscribing yield locus (lines) and FE predictions (symbols) are shown as a function of $\bar{h}$ for two values of $\bar{c}$.

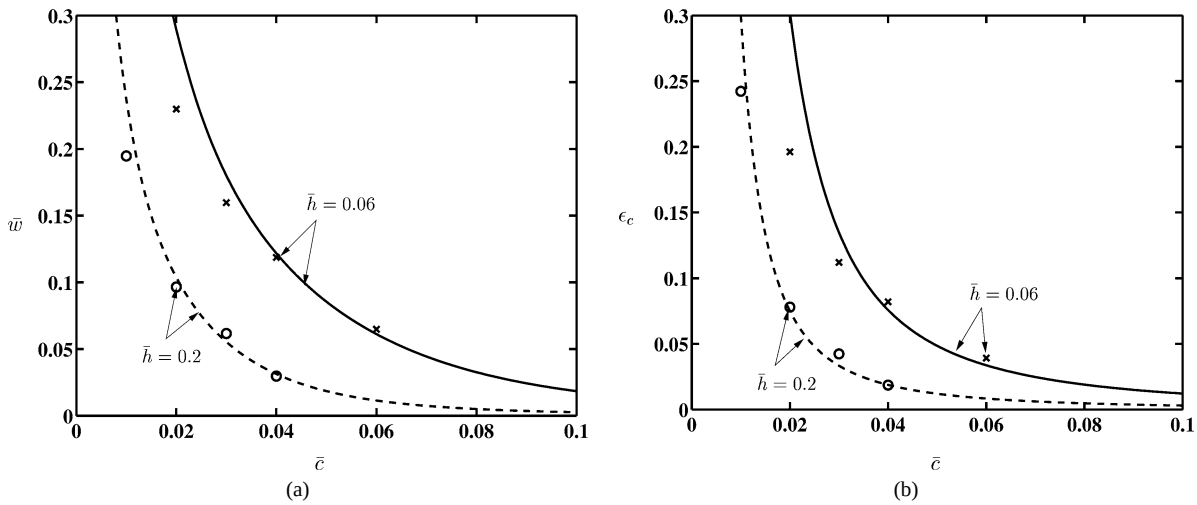

Fig. 7. A comparison between analytical and FE predictions of the (a) maximum deflection $\overline{w}$ at the mid-span of the inner face sheet and (b) core compression ε_c of sandwich beams with reference material properties subject to a normalised impulse $\bar{I} = 10^{-3}$. Analytical predictions employing the inscribing yield locus (lines) and FE predictions (symbols) are shown as a function of $\bar{c}$ for two values of $\bar{h}$.

the outer face sheet at the supports and thus to a loss in momentum. This effect is not accounted for in the analytical model and consequently the analytical model overpredicts the deflections and core compression at high values of impulse.

Comparisons of the analytical and FE predictions of the normalised structural response time $\overline{T}$ and the core compression time $\overline{T}_c$ as functions of $\bar{I}$ are shown in Fig. 9 for the sandwich beam with $\bar{c} = 0.03$ and $\bar{h} = 0.1$. Good agreement between the analytical and FE predictions is seen for the core compression time and, similar to the case of the monolithic beam, the circumscribing yield locus model is in good agreement with the FE predictions of the structural response time. More importantly, the normalised core compression time $\overline{T}_c$ is at-least an order of magnitude smaller than the structural response time $\overline{T}$; this supports the assumption of a separation of time scales for the core compression phase and the beam bending and stretching phase in the analytical model of Fleck and Deshpande (2003).

Effect of elasticity. The analytical predictions assume a rigid perfectly-plastic material response. In the above numerical calculations, the face sheet and core were assumed to possess a yield strain of $\varepsilon_{fY} = \varepsilon_{cY} = 0.2\%$. Here, we investigate the effect of material elasticity on the sandwich beam response by increasing the yield strain to $\varepsilon_{fY} = \varepsilon_{cY} = 0.5\%$ for the

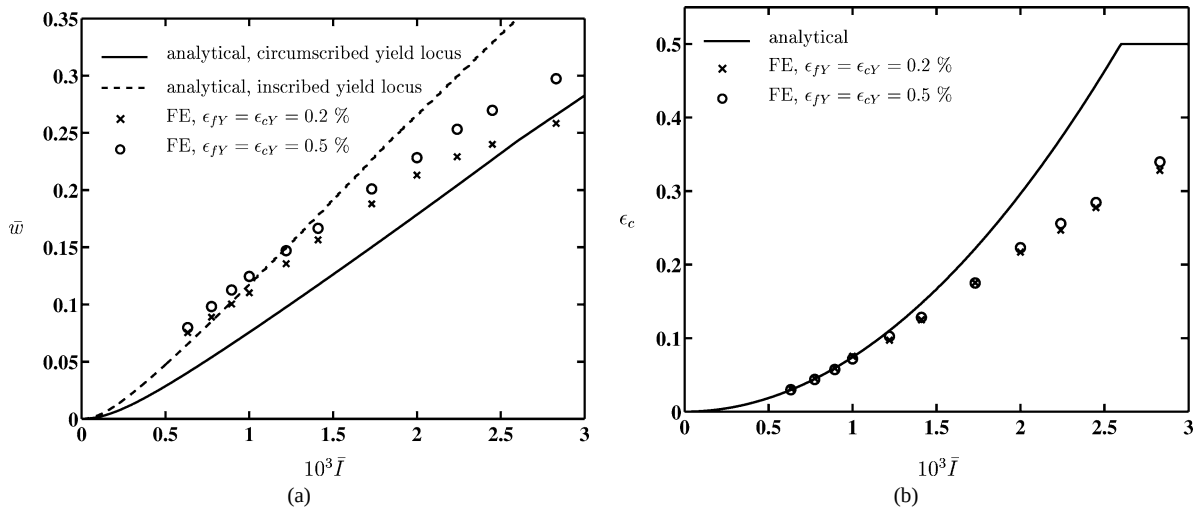

Fig. 8. A comparison between analytical and FE predictions of the (a) maximum deflection $\overline{w}$ at the mid-span of the inner face sheet and (b) core compression ε_c as a function of the applied impulse for sandwich beams with $\bar{c} = 0.03$ and $\bar{h} = 0.1$ made from the reference materials. Results are shown for two selected values of yield strains of the face sheet material and core.

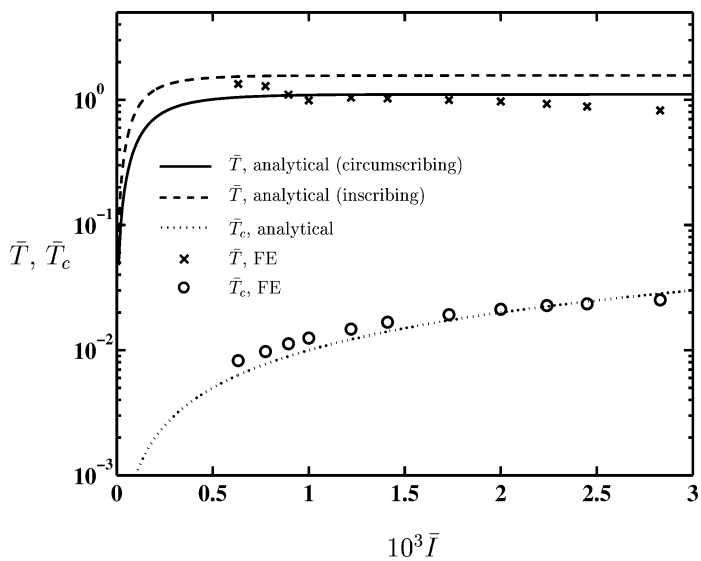

Fig. 9. A comparison between analytical and FE predictions of the structural response time $\overline{T}$ and core compression time $\overline{T_c}$ as a function of the applied impulse for sandwich beams with $\bar{c} = 0.03$ and $\bar{h} = 0.1$ made from the reference materials.

sandwich beam with $\bar{c} = 0.03$ and $\bar{h} = 0.1$. The normalised maximum deflection $\overline{w}$ and core compression ε_c of the sandwich beam with $\varepsilon_{fY} = \varepsilon_{cY} = 0.5\%$ are included in Figs. 8(a) and 8(b), respectively. A comparison with the reference material case ($\varepsilon_{fY} = \varepsilon_{cY} = 0.2\%$) reveals that the deflection $\overline{w}$ increases by not more than 10% while the core compression is negligibly affected. Similarly, the core compression time T_c and structural response time T are not appreciably affected by this increase in yield strain; these results are not included in Fig. 9 as they almost overlap with the FE predictions for $\varepsilon_{fY} = \varepsilon_{cY} = 0.2\%$. In summary, there is no significant effect of material elasticity upon the sandwich beam response for yield strains representative of most structural alloys.

Effect of strain hardening. The analytical models discussed in Section 2 and the FE calculations detailed above both assume ideally-plastic face sheet materials. On the other hand, structural alloys, which are expected to be employed in shock resistant sandwich construction can have a strong strain hardening response. The effect of strain hardening of the face sheet material on the sandwich beam response is investigated here. The face sheet material is assumed to be made from a elastic plastic

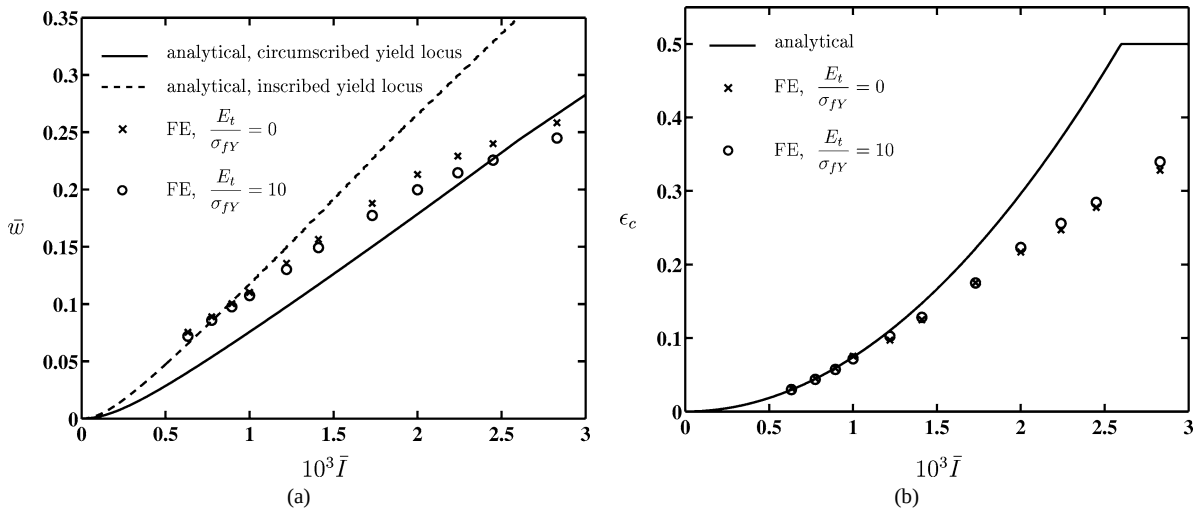

Fig. 10. A comparison between analytical and FE predictions of the (a) maximum deflection $\overline{w}$ of the mid-span of the inner face sheet and (b) core compression ε_c as a function of the applied impulse for sandwich beams with $\bar{c} = 0.03$ and $\bar{h} = 0.1$ made from the reference materials and strain hardening face sheets.

material with yield stress and strain $\sigma_{fY} = 500$ MPa and $\varepsilon_{fY} = 0.2\%$, respectively and a density $\rho_f = 8000$ kg·m^{-3}. The strain hardening response is assumed to be linear with a tangent modulus $E_t/\sigma_{fY} = 10$; this strain hardening is representative of the AL6XN stainless steel. The core properties are unchanged from the reference material case.

Consider a sandwich beam with core made from the reference material and strain hardening face sheets, with geometry $\bar{c} = 0.03$ and $\bar{h} = 0.1$. The normalised maximum deflection $\overline{w}$ is plotted against $\bar{I}$ in Fig. 10. For comparison purposes the deflections of the sandwich beam made from the reference materials with ideally plastic face sheets are included in this figure by re-plotting the data shown in Fig. 8. The strain hardening response of the face sheets is seen to have only a small influence upon the deflection of the sandwich beam. This can be rationalised by recalling that the longitudinal strain in the face sheets is $\varepsilon \approx 0.5\overline{w}^2 \approx 4.5\%$ for $\overline{w} \approx 0.3$. This level of straining does not increase the yield strength of the face sheet material appreciably for the strain hardening considered here and hence the response is insensitive to the strain hardening behaviour of the face sheet material. This conclusion should be moderated for the case of annealed face sheets for which the flow strength at a uniaxial strain of 4.5 % may be significantly above the yield strength.

Effect of core strength. In the calculations detailed above, the core strength was kept constant. Here we investigate the effect of core strength on the sandwich beam response. Results are presented for sandwich beams of geometry $\bar{c} = 0.03$, $\bar{h} = 0.1$ subject to a normalised impulse $\bar{I} = 10^{-3}$. Other than the core strength, the material properties of the sandwich beams were unchanged from the reference material properties. The normalised core strength $\bar{\sigma}$ was varied from 0.01 to 0.08, with a densification strain ε_D held fixed at 0.5; cores weaker than $\bar{\sigma} = 0.01$ were not considered as numerical difficulties were encountered in such cases.

The maximum normalised deflection of the inner face of the sandwich beams $\overline{w}$ is plotted against the normalised core strength $\bar{\sigma}$ in Fig. 11. The FE results indicate that $\overline{w}$ is relatively insensitive to the core strength. Analytical predictions of $\overline{w}$ employing the inscribing and circumscribing yield surfaces are included in Fig. 11; the analytical model employing the inscribing yield surface agrees reasonably well with the FE predictions for beams with the high core strength but overpredicts the deflection of the beams with the weaker cores. Time histories of the plastic dissipation of the entire sandwich beam and only of the core, normalised by the initial kinetic energy of the outer face sheet of the sandwich beam are shown in Fig. 12(a). These curves reveal two stages of deformation. In the first stage, plastic dissipation occurs primarily in the core, with the outer face sheet flying into the core and crushing it; at the end of this stage both face sheets are moving at approximately the same velocity. Subsequently, there is a "knee" in the plastic dissipation curves and plastic dissipation primarily within the face sheets, with the dissipation in the core increasing only gradually with time. It is worth noting that the plastic dissipation in the core at the end of the first stage is nearly independent of the core strength. Further, this stage lasts longer for the weaker cores. Consequently, the separation of time scales between the core compression and beams bending and stretching phases assumed in the analytical model is less accurate for the beams with a weak core.

Finite element predictions of the plastic dissipation at the end of the first stage in the deformation (i.e., the plastic dissipation corresponding to the "knee" in the plastic dissipation versus times curves of Fig. 12(a)) are shown in Fig. 12(b) as a function of the mass ratio $\hat{\rho} = \rho_c c/(\rho_f h)$, for the choices of core strength $\bar{\sigma} = 0.04$ and $\bar{\sigma} = 0.01$. These calculations were conducted on

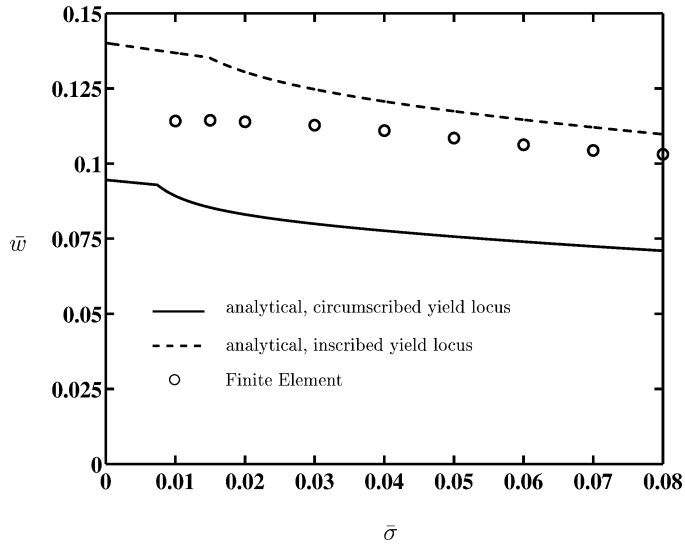

Fig. 11. A comparison between analytical and FE predictions of the maximum deflection $\overline{w}$ at mid-span of the inner face sheet of sandwich beams with $\bar{c} = 0.03$ and $\bar{h} = 0.1$ subject to a normalised impulse $\bar{I} = 10^{-3}$ as a function of the normalised core strength $\bar{\sigma}$.

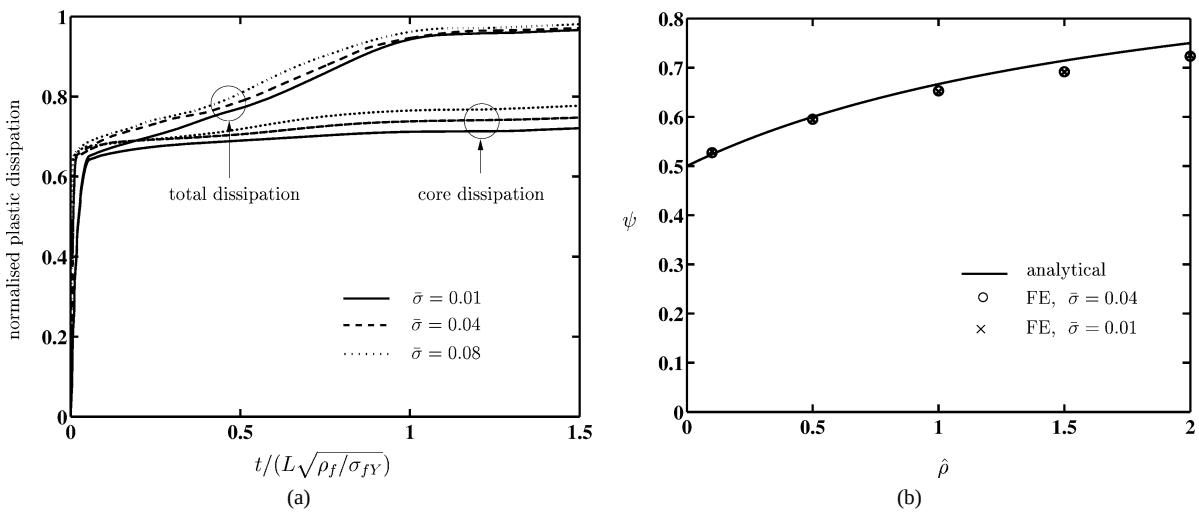

Fig. 12. (a) FE predictions of the time histories of the normalised plastic dissipation in sandwich beams for three selected core strengths. (b) Ratio ψ of the plastic dissipation in the core compression stage to the initial kinetic energy of the outer face as a function of the mass ratio $\hat{\rho}$ for two selected core strengths. The sandwich beams in both cases have geometry $\bar{c} = 0.03$ and $\bar{h} = 0.1$ and were subject to an impulse $\bar{I} = 10^{-3}$.

beams with the above geometry subject to a normalised impulse $\bar{I} = 10^{-3}$. The ratio $\hat{\rho}$ was varied by changing the density of the core material from 80 kg·m^{-3} to 1600 kg·m^{-3}. The figure reveals that the plastic dissipation at the end of the core compression stage is independent of the core strength and increases with $\hat{\rho}$, in excellent agreement with the analytical predictions.

Failure of the sandwich beams. It is difficult to give a precise failure criterion for the beam as it is anticipated that the shock impulse for incipient failure is sensitive to the details of the built-in end conditions of the clamped beams. Thus, the analytical model states a failure criterion based on an estimate of the tensile strain in the face sheets due to uniform stretching of the beam; tensile strains due to bending at the plastic hinges and due to stress concentrations near the supports are neglected.

The deformed profile (at maximum deflection) of sandwich beams with geometry $\bar{c} = 0.03$ and $\bar{h} = 0.1$ made from the reference materials and subject to normalised shock impulses $\bar{I} = 3.2 \times 10^{-3}$ and $\bar{I} = 10^{-3}$ are shown in Fig. 13(a). The deformed profile of the beam resulting from the higher shock impulse distinctly shows a large reduction in its cross-section due to core compression. This high degree of core compression is expected to result in high tensile strains in the outer face near

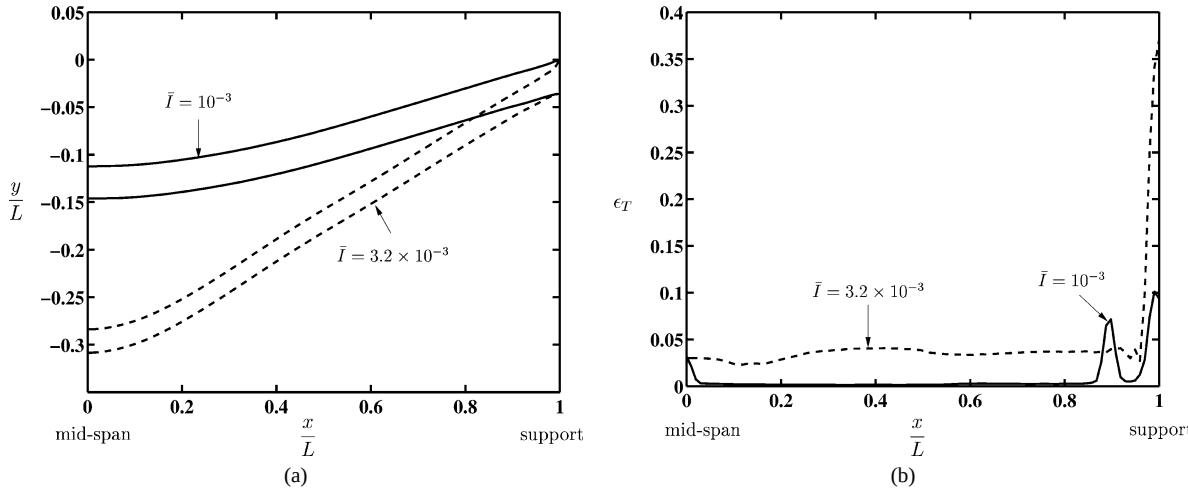

Fig. 13. (a) Deformed profiles of sandwich beams ($\bar{c} = 0.03$, $\bar{h} = 0.1$) made from the reference materials. (b) The maximum principal tensile strains along the length of the outer face sheet at the point of maximum deflection.

the supports. The variation of the maximum principal tensile strain ε_T along the length x of the outer face sheet of the beam at the point of maximum deflection is plotted in Fig. 13(b) for the two levels of impulse considered. In the central section of the beam, ε_T is approximately equal to $0.5\overline{w}^2$ as assumed in the analytical model. However, the strains in the outer face sheet are extremely high near the supports; this is especially so in the high impulse case where substantial core compression occurs. Thus, it is expected that tensile failure of the outer face sheet near the supports will occur at impulse levels much lower than that assumed by the analytical model. Additional investigations are required to establish an appropriate failure criterion for the sandwich beams.

4. Conclusions

Detailed comparisons between finite element (FE) and analytical predictions of the response of sandwich and monolithic clamped beams subject to shock loading have been presented. The main findings include:

1. Impulsive loading suffices to model the shock loading of sandwich structures for most realistic shock pressure versus time histories.
2. The separation of time scales between the core compressions and beam bending stretching phases of the sandwich beams response is borne out by the FE calculations.
3. The analytical model employing the inscribing yield surface is agrees well with the FE predictions of the sandwich beam deflections over a wide range of sandwich beam geometries, shock impulses and material properties.
4. For realistic levels of the beam deflections, strain hardening which is representative of most structural alloys, has a negligible effect upon the sandwich beam response.
5. The FE calculations predict that the compressive strength of the core has a small effect on the sandwich beam response, in support of the analytical model.
6. The FE simulations indicate that high tensile strains develop in the outer face sheets near the supports. This strain concentration is not modelled in the analysis of Fleck and Deshpande (2003) and is expected to govern the failure of the sandwich beams. This topic warrants further investigation.

Acknowledgements

The authors are grateful to ONR for their financial support through US-ONR IFO grant number N00014-03-1-0283 on the Science and Design of Blast Resistant Sandwich Structures. We are pleased to acknowledge Profs. M.F. Ashby, T. Belytschko, A.G. Evans and J.W. Hutchinson for many insightful discussions during the course of this work.

References

Cole, R.H., 1948. Underwater Explosions. Princeton University Press.

Deshpande, V.S., Fleck, N.A., 2000. Isotropic constitutive models for metallic foams. J. Mech. Phys. Solids 48 (6–7), 1253–1283.

Deshpande, V.S., Fleck, N.A., 2001. Collapse of truss core sandwich beams in 3-point bending. Int. J. Solids Structures 38 (36–37), 6275–6305.

Fleck, N.A., Deshpande, V.S., 2003. The resistance of clamped sandwich beams to shock loading. J. Appl. Mech., in press.

Jones, N., 1971. A theoretical study of the dynamic plastic behaviour of beams and plates with finite deflections. Int. J. Solids Structures 7, 1007–1029.

Jones, N., 1989. Structural Impact. Cambridge University Press.

Swisdak, M.M., 1978. Explosion effects and properties: Part II – explosion effects in water, Technical Report, Naval Surface Weapons Center, Dahlgren, Virginia, USA.

Symmonds, P.S., 1954. Large plastic deformations of beams under blast type loading. In: Proceedings of the Second US National Congress of Applied Mechanics, pp. 505–515.

Taylor, G.I., 1941. The pressure and impulse of submarine explosion waves on plates. In: The Scientific Papers of G.I. Taylor, Vol. III. Cambridge University Press. 1963, pp. 287–303.

Wang, A.J., Hopkins, H.G., 1954. On the plastic deformation of built-in circular plates under impulsive load. J. Mech. Phys. Solids 3, 22–37.

Xue, Z., Hutchinson, J.W., 2003. A comparative study of blast-resistant metal sandwich plates. Int. J. Impact Engrg., submitted for publication.